

Search for the rare decay $J/\psi \rightarrow \gamma D^0 + \text{c.c.}$ at BESIII

M. Ablikim *et al.**
(BESIII Collaboration)

 (Received 21 August 2024; accepted 14 November 2024; published 13 December 2024)

Using $(10087 \pm 44) \times 10^6 J/\psi$ events collected with the BESIII detector, we search for the rare decay $J/\psi \rightarrow \gamma D^0 + \text{c.c.}$ for the first time. No significant signal is observed and the upper limit on the branching fraction is determined to be $\mathcal{B}(J/\psi \rightarrow \gamma D^0 + \text{c.c.}) < 9.1 \times 10^{-8}$ at 90% confidence level.

DOI: [10.1103/PhysRevD.110.112012](https://doi.org/10.1103/PhysRevD.110.112012)

I. INTRODUCTION

Search for physics beyond the Standard Model (SM) is one of the major tasks in particle physics. Weak decays of the charmonium state J/ψ are an excellent probe of potential new Physics (NP) effects. In the SM, a J/ψ can weakly decay through flavor changing charged currents (FCCCs), allowed at tree level, producing a single charm meson alongside other noncharmed mesons or leptons. These decays have branching fractions (BFs) in the range of 10^{-9} to 10^{-11} in the SM [1–7]. Many NP models predict an enhancement of these BFs by 2 or 3 orders of magnitude [8–10]. Therefore, extensive studies of these BFs in the BESIII experiment [11–14] can constrain the parameter space of various models.

In addition, the weak decay of J/ψ mediated by a flavor changing neutral current (FCNC) is another interesting process. While prohibited at the tree level, it can occur via $c \rightarrow u$ transition at the loop level in the SM but is highly suppressed due to the Glashow-Iliopoulos-Maiani (GIM) mechanism [15]. Such decays can also occur via long-distance effects, which are expected to have the same order of magnitude as the production rate of the FCNC process [16]. The FCNC decay $J/\psi \rightarrow D^0 l^+ l^-$, within the SM framework, is anticipated to have a BF of the order of 10^{-13} [16]. In comparison, the FCNC process $J/\psi \rightarrow \gamma D^0$ (the charged conjugate channel is always implied throughout the text), as depicted in Fig. 1, is expected with a 1 or 2 orders of magnitude larger BF, due to the presence of one fewer decay vertex. The experimental evidence for this FCNC process provides an opportunity to study the non-perturbative QCD effects and their underlying dynamics.

Any enhancement of the BF with respect to the SM would be a strong indication of NP [17,18].

Experimentally, the FCNC processes have been comprehensively studied in the B meson sector via $b \rightarrow s$ transitions [19,20] and in the $D_{(s)}$ meson sector via $c \rightarrow u$ transitions [21–25]. So far, they have not been observed in the charm sector. The $c \rightarrow u\gamma$ transition can be directly probed by studying the radiative decay $J/\psi \rightarrow \gamma D^0$. In 2017, the BESIII experiment searched for $J/\psi \rightarrow D^0 e^+ e^-$ [26] using $(1310.6 \pm 7.2) \times 10^6 J/\psi$ events resulting in an upper limit on the BF $< 8.5 \times 10^{-8}$ at 90% confidence level (C.L.).

In this paper, we search for $J/\psi \rightarrow \gamma D^0$ based on $(10087 \pm 44) \times 10^6 J/\psi$ events [27] collected by the BESIII detector. This is the world's largest J/ψ sample produced at an electron-positron collider. Its clean environment provides an excellent opportunity to search for this rare decay. To study the decay $J/\psi \rightarrow \gamma D^0$, the D^0 is reconstructed through its three prominent exclusive hadronic decay modes, $K^- \pi^+$ (mode I), $K^- \pi^+ \pi^0$ (mode II), and $K^- \pi^+ \pi^+ \pi^-$ (mode III), which have large BFs. The semi-blind analysis strategy is adopted, where the selection criteria are determined using 10% of the data sample, and the final results are obtained using the full data sample.

II. BESIII DETECTOR AND MONTE CARLO SIMULATION

The BESIII detector [28] records symmetric e^+e^- collision events provided by the BEPCII storage ring [29] in the center-of-mass energy ranging from 1.84 to

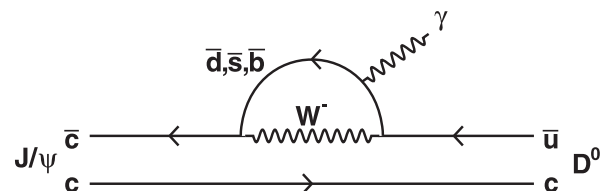


FIG. 1. Feynman diagram for $J/\psi \rightarrow \gamma D^0$.

*Full author list given at the end of the article.

Published by the American Physical Society under the terms of the [Creative Commons Attribution 4.0 International license](https://creativecommons.org/licenses/by/4.0/). Further distribution of this work must maintain attribution to the author(s) and the published article's title, journal citation, and DOI. Funded by SCOAP³.

4.95 GeV, with an achieved peak luminosity of $1.1 \times 10^{33} \text{ cm}^{-2} \text{ s}^{-1}$ at $\sqrt{s} = 3.773 \text{ GeV}$. BESIII has collected large data samples in this energy region [30]. The cylindrical core of the BESIII detector covers 93% of the full solid angle and consists of a helium-based multilayer drift chamber (MDC), a plastic scintillator time-of-flight system (TOF), and a CsI(Tl) electromagnetic calorimeter (EMC), which are all enclosed in a superconducting solenoidal magnet providing a 1.0 T magnetic field. The magnetic field was 0.9 T in 2012, which affects 11% of the total J/ψ data. The solenoid is supported by an octagonal flux-return yoke with resistive plate counter muon identification modules interleaved with steel. The momentum resolution of charged-particle at 1 GeV/ c is 0.5%, and the dE/dx resolution is 6% for electrons from Bhabha scattering. The EMC measures photon energies with a resolution of 2.5% (5%) at 1 GeV in the barrel (end cap) region. The time resolution in the TOF barrel region is 68 ps, while that in the end cap region is 110 ps. The end cap TOF system was upgraded in 2015 using multigap resistive plate chamber technology, providing a time resolution of 60 ps, which benefits 87% of the data used in this analysis [31–33].

Simulated data samples produced with a Geant4-based [34] Monte Carlo (MC) package, which includes the geometric description of the BESIII detector and the detector response, are used to determine the detection efficiencies and to estimate backgrounds. In the simulation, the beam energy spread and initial state radiation in the e^+e^- annihilations are modeled with the generator KKMC [35]. An inclusive MC sample of 10^{10} J/ψ events, including the production of the J/ψ resonance, is generated to study the backgrounds. All particle decays are modeled either with EvtGen [36,37] using BFs taken from the Particle Data Group (PDG) [38], when available, or otherwise estimated with the LUNDCHARM [39,40] package. Final state radiation from charged final state particles is incorporated using the PHOTOS package [41]. To estimate the detection efficiency, the signal events of $J/\psi \rightarrow \gamma D^0$ are generated by the JPE model [42] which is constructed for a vector meson decays into a photon plus a pseudoscalar meson, with the phase space model for $D^0 \rightarrow K^- \pi^+$ and the model from the amplitude analyses for $D^0 \rightarrow K^- \pi^+ \pi^0$ and $D^0 \rightarrow K^- \pi^+ \pi^+ \pi^-$ [43].

III. DATA ANALYSIS

A. Common selection

Charged tracks reconstructed in the MDC are required to be within a polar angle (θ) range of $|\cos \theta| < 0.93$, where θ is defined with respect to the z -axis, which is the symmetry axis of the MDC. The distance of closest approach to the interaction point (IP) must be less than 10 cm along the z -axis, and less than 1 cm in the transverse plane. Particle identification (PID) is carried out for charged tracks by combining the specific ionization energy loss measured by the MDC (dE/dx) and the flight time in the TOF to form

the likelihoods $\mathcal{L}(h)$ for the $h = K, \pi$ hypotheses. Charged kaons and pions are identified by requiring $\mathcal{L}(K) > \mathcal{L}(\pi)$ and $\mathcal{L}(\pi) > \mathcal{L}(K)$, respectively.

Photon candidates are identified by using showers in the EMC. The deposited energy of each shower must be more than 25 MeV in the barrel region ($|\cos \theta| < 0.80$) and more than 50 MeV in the end cap region ($0.86 < |\cos \theta| < 0.92$). To exclude showers originating from charged tracks, the opening angle subtended by the EMC shower and the position of the closest charged track at the EMC must be greater than 20° as measured from the IP. To suppress electronic noise and showers unrelated to the event, the difference between the EMC time and the event start time is required to be within $[0, 700]$ ns. The π^0 candidates are reconstructed with pairs of selected photons. The invariant mass of the photon pair is required to be within $[0.115, 0.150]$ GeV/ c^2 . To improve the kinematic resolution, a kinematic fit [44] is carried out, constraining the invariant mass of the photon pair to be the π^0 nominal mass [38], and the corresponding χ^2 of the kinematic fit is required to be less than 20.

The candidate events are selected by requiring a radiative photon from J/ψ decay, the charged track of a kaon, and one or three charged pions or additionally a neutral pion (depending on the D^0 decay modes). The radiative photon with the maximum energy is selected and the charged tracks are required to have zero net charge. All three modes require to have no additional charged track, and mode II requires one π^0 candidate. To improve the resolution and reduce the backgrounds, a four-constraint (4C) kinematic fit is performed, imposing energy-momentum conservation under the hypothesis of $J/\psi \rightarrow K^- \pi^+ \gamma$ for mode I or $J/\psi \rightarrow K^- \pi^+ \pi^+ \pi^- \gamma$ for mode III. Alternatively, a five-constraint (5C) kinematic fit is carried out under the hypothesis of $J/\psi \rightarrow K^- \pi^+ \gamma \gamma$ for mode II, with an additional constraint on the $\gamma\gamma$ invariant mass to match the π^0 nominal mass. For the fit, $\chi_{4C/5C}^2 < 30$ is required. For events with more than one π^0 candidate in mode II, the one with the minimum χ_{5C}^2 value is retained for further analysis. The momenta of the charged tracks and the showers after the kinematic fit are used for further analysis throughout the text if not mentioned explicitly.

B. Further selection

For mode I, the dominant backgrounds are $J/\psi \rightarrow \pi^+ \pi^- \gamma$, $J/\psi \rightarrow K^+ K^- \gamma$, and $J/\psi \rightarrow \pi^+ \pi^- \pi^0$, due to the misidentification between a high momentum kaon and a pion, or due to missing a soft photon. To remove these backgrounds, 4C kinematic fits under the hypotheses of $J/\psi \rightarrow \pi^+ \pi^- \gamma$, $J/\psi \rightarrow K^+ K^- \gamma$ and $J/\psi \rightarrow \pi^+ \pi^- \gamma \gamma$ (named as alternative kinematic fit1/fit2/fit3, similarly named for mode II and III) are carried out demanding $\chi_{\pi^+ \pi^- \gamma / K^+ K^- \gamma / \pi^+ \pi^- \gamma \gamma}^2 > 85/50/35$. These requirements have been optimized by maximizing the quantity of Punzi figure

of merit (FOM) $\epsilon/(1.5 + \sqrt{B})$ [45] (analogously employed in the similar event selection), where ϵ is the signal efficiency and B is the background yield. After these selections, the momentum requirements, $p_{K/\pi} < 1.25/1.35 \text{ GeV}/c$, are applied to suppress the backgrounds from K/π misidentification. Other backgrounds from radiative Bhabha and dimuon events occur due to misidentifying leptons as hadrons and their large cross sections. To suppress the radiative Bhabha background, the requirement of $E/p < 0.8$ is applied for any charged pion candidate, where E and p are the corresponding energy deposited in the EMC and the momentum measured in the MDC, respectively. The requirement of $\chi_{\pi^+\pi^-\gamma}^2 > 85$ suppresses the radiative dimuon background.

For mode II, the dominant background is $J/\psi \rightarrow K^-\pi^+\pi^0\pi^0$ with the intermediate process $K_S^0 \rightarrow \pi^0\pi^0$ with a missing soft photon. A mass window $0.32 < M_{K^-\pi^+}^{\text{Recoil}} < 0.66 \text{ GeV}/c^2$ is applied to veto this background, where $M_{K^-\pi^+}^{\text{Recoil}}$ is the recoil mass of the $K^-\pi^+$ system calculated with the $K^-\pi^+$ momenta before the kinematic fit. There are also backgrounds from $J/\psi \rightarrow \pi^+\pi^-\pi^0\gamma$ (including $\omega \rightarrow \gamma\pi^0$), $J/\psi \rightarrow K^+K^-\pi^0\gamma$, and $J/\psi \rightarrow \pi^+\pi^-\pi^0\pi^0(\gamma\gamma)$ due to the misidentification between a high momentum kaon and a pion, or due to missing a soft photon. To suppress these backgrounds, 4C kinematic fits under the hypotheses of $J/\psi \rightarrow \pi^+\pi^-\gamma\gamma\gamma$, $J/\psi \rightarrow K^+K^-\gamma\gamma\gamma$ and $J/\psi \rightarrow \pi^+\pi^-\gamma\gamma\gamma\gamma$ are performed and $\chi_{\pi^+\pi^-\pi^0\gamma/K^+K^-\pi^0\gamma/\pi^+\pi^-\pi^0\gamma\gamma}^2 > 40/40/95$ are required, individually. A mass window of the $\gamma\pi^0$ invariant mass, $0.68 < M_{\gamma\pi^0} < 0.92 \text{ GeV}/c^2$, is applied to veto the background from $J/\psi \rightarrow \omega\pi^+\pi^- \rightarrow \pi^+\pi^-\pi^0\gamma$. Another potential background is $J/\psi \rightarrow K^+K^-\gamma$ due to the charged kaon decay $K^+ \rightarrow \pi^+\pi^0$. A mass window is applied to the $\pi^+\pi^0$ invariant mass with $0.45 < M_{\pi^+\pi^0} < 0.53 \text{ GeV}/c^2$ to veto this background. The background with $J/\psi \rightarrow K^-\pi^+\pi^0K_L^0$ also presents in the case of a K_L^0 shower in the EMC misidentified as the radiative photon candidate. To veto this background, a multivariate data analysis (MVA) in the ROOT TMVA package [46] is performed on the shower shape in the EMC based on a gradient boosted decision trees (BDTG) algorithm. The input parameters in the MVA include N_{hit} (the number of hit crystals in the EMC), $E_{\text{seed}}/E_{3\times 3}$ (ratio of energy deposited in the center crystal of the shower to that in the 3×3 crystals), $E_{3\times 3}/E_{5\times 5}$ (ratio of energy deposited in the 3×3 crystals to that in the 5×5 crystals) and A_{42} moment as defined in Ref. [47] with relatively small correlation. In order to train and test the MVA, the photon candidates from the exclusive signal MC sample and the K_L^0 candidates from the exclusive MC sample of $J/\psi \rightarrow K^-\pi^+\pi^0K_L^0$ are used. By applying the MVA method on the surviving events of inclusive and signal MC samples, the K_L^0 background is suppressed by 90% with the requirement of the BDTG output value while keeping 98.4% signal efficiency.

For mode III, the dominant background is $J/\psi \rightarrow K^-\pi^+\pi^+\pi^-\gamma(\pi^0)$ with a $\pi^+\pi^-$ pair from K_S^0 decay (missing a soft photon). Therefore a mass window $0.46 < M_{\pi^+\pi^-} < 0.55 \text{ GeV}/c^2$ is applied to veto this background, where $M_{\pi^+\pi^-}$ is the invariant mass of any $\pi^+\pi^-$ pair (two pairs per event). Another main background contribution is $J/\psi \rightarrow \pi^+\pi^-\pi^+\pi^-\gamma$ due to the misidentification between a high momentum kaon and a pion. A 4C kinematic fit under the hypothesis of $J/\psi \rightarrow \pi^+\pi^-\pi^+\pi^-\gamma$ is carried out and $\chi_{\pi^+\pi^-\pi^+\pi^-\gamma}^2 > 430$ is required. There are also backgrounds due to charged kaon decay, such as $J/\psi \rightarrow K^+K^-\gamma$ with $K^+ \rightarrow \pi^+\pi^0$ and $J/\psi \rightarrow K^+K^-\pi^+\pi^-$ with $K^+ \rightarrow \pi^+\pi^0$ and a missing soft photon. The corresponding mass windows for the $\pi^+\pi^+\pi^-$ invariant mass $0.47 < M_{\pi^+\pi^+\pi^-} < 0.52 \text{ GeV}/c^2$ and the recoil mass of the $K^-\pi^+\pi^-$ combination with the least deviation from the nominal K mass $0.42 < M_{K^-\pi^+\pi^-}^{\text{Recoil}} < 0.52 \text{ GeV}/c^2$ are applied to veto these backgrounds. Another potential background is $J/\psi \rightarrow K^+K^-\pi^0$ due to the Dalitz decay $\pi^0 \rightarrow e^+e^-\gamma$. To reject this background, a mass window of the $e^+e^-\gamma$ invariant mass (replacing the mass of the pion with that of an electron), $0.09 < M_{e^+e^-\gamma} < 0.19 \text{ GeV}/c^2$, is applied.

C. Signal extraction and branching fraction calculation

After the selection criteria described in Sec. III B have been applied, the invariant mass distributions of the $K^-\pi^+$, $K^-\pi^+\pi^0$ and $K^-\pi^+\pi^+\pi^-$ for the three D^0 decay modes are shown in Fig. 2. The BF of $J/\psi \rightarrow \gamma D^0$ is calculated by

$$B(J/\psi \rightarrow \gamma D^0 + \text{c.c.}) = \frac{N_i^{\text{sig}}}{N_{J/\psi} \times \mathcal{B}_i \times \epsilon_i}, \quad (1)$$

where N_i^{sig} is the signal yield observed in the i th decay mode, $N_{J/\psi}$ is the total number of J/ψ events, \mathcal{B}_i is the corresponding BF of the D^0 decay and its subsequent daughter particles' decays, and ϵ_i is the reconstruction efficiency obtained with the signal MC samples, which is $(22.96 \pm 0.11)\%$, $(14.83 \pm 0.09)\%$, and $(17.55 \pm 0.10)\%$ for modes I, II and III, respectively.

To extract the BF of $J/\psi \rightarrow \gamma D^0$, an unbinned simultaneous maximum-likelihood fit is carried out to the selected samples of the three D^0 decay modes by sharing the same decay BF of $J/\psi \rightarrow \gamma D^0$. In the fit, the signal is described with a pdf based on kernel estimation derived from the signal MC sample, and the background is described by a line with the slope allowed to float. The simultaneous fit results are shown in Fig. 2 with the statistical significance 0.51σ . No obvious signal is observed, therefore an upper limit on the BF of $J/\psi \rightarrow \gamma D^0$ at 90% C.L. is set in Sec. III E.

D. Systematic uncertainties

Several systematic uncertainties are considered in the BF measurement. The uncertainties are separated into two

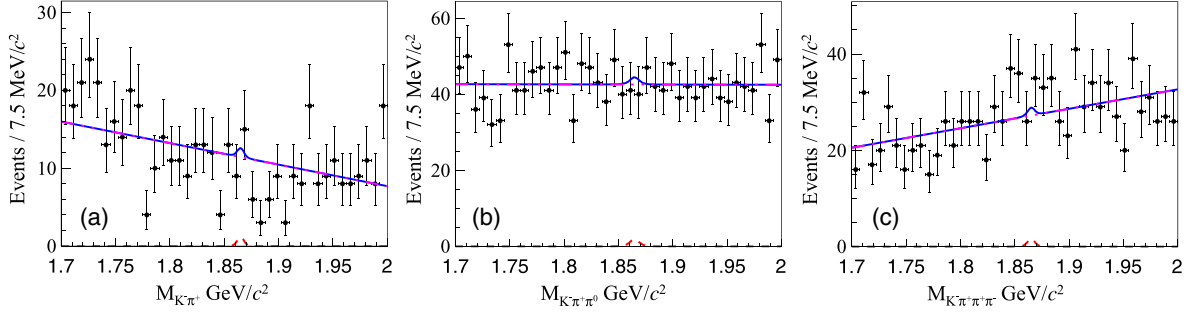


FIG. 2. The unbinned simultaneous fit on the invariant mass distributions of modes (a) I, (b) II and (c) III, where the dots with error bar are data, the blue lines are the fit result, and the red dotted and purple curves are the fitted signal and background, respectively.

categories according to the approaches to evaluate their effects on the BF measurement, 1) effects that are evaluated with the different scenarios (under different selection criteria) and extracted by their resultant differences with respect to the nominal value, named category A thereafter; 2) effects that are evaluated with the various methods, and propagated to the final results directly, named category B thereafter. The sources of systematic uncertainties and the assigned values are summarized in Table I.

The category A uncertainties include those associated with the K/π momentum requirements, the mass window veto requirement as well as the shapes of signal and background in the fit. The uncertainties associated with the K/π

momentum requirements are estimated by changing the boundary by ± 0.005 or ± 0.010 GeV/c based on the nominal values. The different mass windows are applied to veto the backgrounds associated with narrow intermediate states K_S^0 , K , ω and π^0 . The corresponding uncertainties are estimated by varying the mass window boundaries by ± 1 or ± 2 times the corresponding mass resolution. The uncertainties associated with the line shapes of signal and background in the fit are estimated with the alternative line shapes; i.e., the signal shape is parametrized with a double Gaussian function with the parameters extracted from a fit to the signal MC sample, while the background line shape is described with a second-order polynomial function. All above alternative scenarios are carried out, and the scenario yielding the largest difference with respect to the nominal value is finally adopted as the corresponding systematic uncertainties concerned.

The category B uncertainties are those associated with the tracking and PID for the charged tracks, the photon detection and π^0 reconstruction, the E/p ratio, the MVA cut for the radiative photon, the number of extra track requirement, the kinematic fit, the quoted BFs of intermediate states, and the total number of J/ψ events.

To estimate the corresponding uncertainties, the efficiencies of tracking and PID for the pions and kaons are studied with the control samples of $J/\psi \rightarrow \pi^+\pi^-\pi^0$ and $J/\psi \rightarrow K_S^0 K^- \pi^+ \rightarrow K^- \pi^+ \pi^+ \pi^-$, respectively. The efficiencies of photon detection [48], π^0 reconstruction [48] and E/p ratio are studied with control sample of $J/\psi \rightarrow \pi^+\pi^-\pi^0$ individually. All above efficiencies are studied both for the data and for the corresponding MC samples in bins of p and $\cos \theta$. The average relative differences of the efficiencies between data and MC simulation, which are obtained by weighting according to the distribution of signal MC samples, are taken as the systematic uncertainties.

The efficiencies of the number of extra tracks requirement and the MVA cut for the radiative photon are also studied using the control sample of $J/\psi \rightarrow \pi^+\pi^-\pi^0$. The relative differences of the efficiencies between data and MC simulation are taken as the uncertainty. The uncertainty associated with the kinematic fit is mainly due to the

TABLE I. Sources of systematic uncertainties and the corresponding uncertainties to the BF (in %), where “-” denotes not applied, and “*” indicates the category A uncertainties.

Source/mode	I	II	III
Momentum	*	-	-
Veto K_S^0	-	*	*
Veto K decay	-	*	*
Veto ω	-	*	-
Veto π^0	-	-	*
Signal line shape	*	*	*
Background line shape	*	*	*
Tracking	0.6	1.1	2.4
PID	2.0	1.4	1.8
Photon requirement	1.0	1.0	1.0
π^0 selection	-	2.2	-
$N_{\text{extra}} = 0$	0.1	0.1	0.1
Kinematic fit	0.8	0.5	2.0
Alternative kinematic fit1	0.2	0.4	0.8
Alternative kinematic fit2	0.0	0.0	-
Alternative kinematic fit3	0.1	0.1	-
E/p ratio	0.9	-	-
MVA cut	-	0.2	-
Quoted BFs	0.8	4.2	1.7
$N_{J/\psi}$	0.4	0.4	0.4
Total	2.7	5.2	4.1

inconsistency of the kinematic variables of charged tracks. Therefore the kinematic variables of charged tracks of the signal MC sample are smeared to minimize the difference between data and MC simulation, and the resulting change in the detection efficiency is taken as the uncertainty. The systematic uncertainties due to the kinematic fit are estimated for all the signal and background hypotheses individually. The details of smearing parameters of charged tracks can be found in Ref. [49]. The uncertainties of the decay BF of intermediate states are taken from the PDG [38]. The uncertainty of the total number of J/ψ events is taken from Ref. [27].

E. Upper limit on branching fraction

As the data are compatible with a background-only hypothesis, a Bayesian method [50] is utilized to obtain an upper limit at 90% C.L. on the BF of $J/\psi \rightarrow \gamma D^0$. The likelihood values are obtained by performing simultaneous fits on the distributions of the invariant masses of $K^-\pi^+$, $K^-\pi^+\pi^0$, and $K^-\pi^+\pi^+\pi^-$ with different BF hypotheses, as shown in Fig. 3.

To incorporate the effects of category A uncertainties, the alternative simultaneous fits for the three D^0 decay modes are carried out with all different scenarios, as discussed in Sec. III D. The fit with the largest upper limit, with the statistical significance 0.77σ , ensuring the most conservative estimate, is selected for analysis. To further incorporate the category B uncertainties, the simultaneous fit for the three D^0 decay modes is carried out, where the BF is the fitting parameter and the signal efficiencies of the three decay modes are treated as nuisance parameters. The distributions of the signal efficiencies for the three D^0

decay modes are assumed to follow a Gaussian distribution with a mean of the corresponding signal MC efficiency, and a width of the corresponding absolute systematic uncertainties without correlation. For the systematic uncertainties with correlation, such as the uncertainty of $N_{J/\psi}$, a Gaussian distribution with a mean of 1 and the corresponding uncertainty as the standard deviation is incorporated for three decay modes. The profiled likelihood value incorporating the category B uncertainties is shown in Fig. 3.

The upper limit at 90% C.L. on the BF of $J/\psi \rightarrow \gamma D^0$ is $\mathcal{B}(J/\psi \rightarrow \gamma D^0) < 9.1 \times 10^{-8}$ with the systematic uncertainties (6.1×10^{-8} without the systematic uncertainties), obtained by integrating the profile likelihood value from 0 to a definitive value which corresponds to 90% of total area.

IV. SUMMARY

In summary, we have presented the first search for the rare decay $J/\psi \rightarrow \gamma D^0$ using $(10087 \pm 44) \times 10^6$ J/ψ events collected with the BESIII detector. Our results are consistent with a background-only hypothesis, and we establish an upper limit on the branching fraction of $\mathcal{B}(J/\psi \rightarrow \gamma D^0 + \text{c.c.}) < 9.1 \times 10^{-8}$ at 90% C.L., representing the most stringent limit to date. Although our measurement do not reach the precision predicted by the SM, it provides a valuable reference for studying different NP models and restrict the phase space of parameters. The sensitivity of searching for this decay could be improved with a larger J/ψ sample, potentially achievable through future experiments [51].

ACKNOWLEDGMENTS

The BESIII Collaboration thanks the staff of BEPCII and the IHEP computing center and the supercomputing center of the University of Science and Technology of China (USTC) for their strong support. This work is supported in part by National Key R&D Program of China under Contracts No. 2020YFA0406400, No. 2020YFA0406300, No. 2023YFA1606000, No. 2023YFA1609400; National Natural Science Foundation of China (NSFC) under Contracts No. 11625523, No. 11635010, No. 11735014, No. 11935015, No. 11935016, No. 11935018, No. 12025502, No. 12035009, No. 12035013, No. 12061131003, No. 12105276, No. 12122509, No. 12192260, No. 12192261, No. 12192262, No. 12192263, No. 12192264, No. 12192265, No. 12221005, No. 12225509, No. 12235017, No. 12361141819; the Chinese Academy of Sciences (CAS) Large-Scale Scientific Facility Program; the CAS Center for Excellence in Particle Physics (CCEPP); Joint Large-Scale Scientific Facility Funds of the NSFC and CAS under Contracts No. U1832207, No. U2032111,

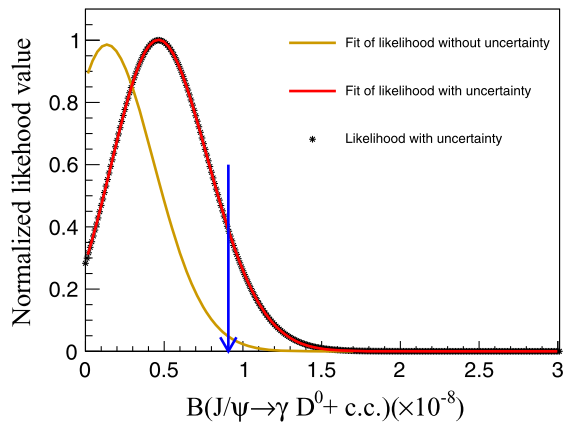


FIG. 3. The likelihood profile for $\mathcal{B}(J/\psi \rightarrow \gamma D^0 + \text{c.c.})$ combining the three decay modes to extract the upper limit on the BF. The black dots are the likelihood distribution with systematic uncertainty, the blue arrow is the 90% integral value of the red line, and the red and orange lines are the curves of the fit results for the likelihood with and without category A and B uncertainties, respectively.

No. U1732263, No. U1832103; CAS Youth Team Program under Contract No. YSBR-101; 100 Talents Program of CAS; The Institute of Nuclear and Particle Physics (INPAC) and Shanghai Key Laboratory for Particle Physics and Cosmology; German Research Foundation DFG under Contracts No. 455635585, No. FOR5327, No. GRK 2149; Istituto Nazionale di Fisica Nucleare, Italy; Ministry of Development of Turkey under Contract No. DPT2006K-120470; National Research Foundation of Korea under Contract No. NRF-2022R1A2C1092335;

National Science and Technology fund of Mongolia; National Science Research and Innovation Fund (NSRF) via the Program Management Unit for Human Resources & Institutional Development, Research and Innovation of Thailand under Contract No. B16F640076; Polish National Science Centre under Contract No. 2019/35/O/ST2/02907; The Swedish Research Council; U.S. Department of Energy under Contract No. DE-FG02-05ER41374.

-
- [1] M. A. Sanchis-Lozano, *Z. Phys. C* **62**, 271 (1994).
 [2] Y.-M. Wang, H. Zou, Z.-T. Wei, X.-Q. Li, and C.-D. Lu, *Eur. Phys. J. C* **54**, 107 (2008).
 [3] Y.-L. Shen and Y.-M. Wang, *Phys. Rev. D* **78**, 074012 (2008).
 [4] R. Dhir and R. C. Verma, *Adv. High Energy Phys.* **2013**, 706543 (2013).
 [5] M. A. Ivanov and C. T. Tran, *Phys. Rev. D* **92**, 074030 (2015).
 [6] T. Wang, Y. Jiang, H. Yuan, K. Chai, and G.-L. Wang, *J. Phys. G* **44**, 045004 (2017).
 [7] Z.-J. Sun, Z.-Q. Zhang, Y.-Y. Yang, and H. Yang, *Eur. Phys. J. C* **84**, 65 (2024).
 [8] C. T. Hill, *Phys. Lett. B* **345**, 483 (1995).
 [9] C. Aulakh and R. Mohapatra, *Phys. Lett.* **119B**, 136 (1982).
 [10] S. L. Glashow and S. Weinberg, *Phys. Rev. D* **15**, 1958 (1977).
 [11] M. Ablikim *et al.* (BESIII Collaboration), *Phys. Rev. D* **110**, 032020 (2024).
 [12] M. Ablikim *et al.* (BESIII Collaboration), *J. High Energy Phys.* **06** (2021) 157.
 [13] M. Ablikim *et al.* (BESIII Collaboration), *J. High Energy Phys.* **01** (2024) 126.
 [14] Z. Li and Z. You, [arXiv:2403.11597](https://arxiv.org/abs/2403.11597).
 [15] S. L. Glashow, J. Iliopoulos, and L. Maiani, *Phys. Rev. D* **2**, 1285 (1970).
 [16] Y.-M. Wang, H. Zou, Z.-T. Wei, X.-Q. Li, and C.-D. Lü, *J. Phys. G* **36**, 105002 (2009).
 [17] X. Zhang, [arXiv:hep-ph/0010105](https://arxiv.org/abs/hep-ph/0010105).
 [18] A. Datta, P. J. O'Donnell, S. Pakvasa, and X. Zhang, *Phys. Rev. D* **60**, 014011 (1999).
 [19] C. Marin Benito (LHCb Collaboration), *Proc. Sci. Lepton-Photon2019* (2019) 014.
 [20] G. de Marino (Belle and Belle-II Collaboration), *Proc. Sci. FPCP2023* (2023) 008.
 [21] M. Ablikim *et al.* (BESIII Collaboration), *Phys. Rev. D* **97**, 072015 (2018).
 [22] R. Aaij *et al.* (LHCb Collaboration), *J. High Energy Phys.* **06** (2021) 044.
 [23] J. P. Lees *et al.* (BABAR Collaboration), *Phys. Rev. D* **84**, 072006 (2011).
 [24] M. Ablikim *et al.* (BESIII Collaboration), *Phys. Rev. D* **105**, L071102 (2022).
 [25] M. Ablikim *et al.* (BESIII Collaboration), *Phys. Rev. Lett.* **133**, 121801 (2024).
 [26] M. Ablikim *et al.* (BESIII Collaboration), *Phys. Rev. D* **96**, 111101 (2017).
 [27] M. Ablikim *et al.* (BESIII Collaboration), *Chin. Phys. C* **46**, 074001 (2022).
 [28] M. Ablikim *et al.* (BESIII Collaboration), *Nucl. Instrum. Methods Phys. Res., Sect. A* **614**, 345 (2010).
 [29] C. Yu *et al.*, in *Proceedings of the 7th International Particle Accelerator Conference* (2016), p. TUYA01.
 [30] M. Ablikim *et al.* (BESIII Collaboration), *Chin. Phys. C* **44**, 040001 (2020).
 [31] X. Li *et al.*, *Radiat. Detect. Technol. Methods* **1**, 13 (2017).
 [32] Y.-X. Guo *et al.*, *Radiat. Detect. Technol. Methods* **1**, 15 (2017).
 [33] P. Cao *et al.*, *Nucl. Instrum. Methods Phys. Res., Sect. A* **953**, 163053 (2020).
 [34] S. Agostinelli *et al.* (GEANT4 Collaboration), *Nucl. Instrum. Methods Phys. Res., Sect. A* **506**, 250 (2003).
 [35] S. Jadach, B. F. L. Ward, and Z. Was, *Comput. Phys. Commun.* **130**, 260 (2000).
 [36] D. J. Lange, *Nucl. Instrum. Methods Phys. Res., Sect. A* **462**, 152 (2001).
 [37] R.-G. Ping, *Chin. Phys. C* **32**, 599 (2008).
 [38] R. L. Workman *et al.* (Particle Data Group), *Prog. Theor. Exp. Phys.* **2022**, 083C01 (2022).
 [39] J. C. Chen, G. S. Huang, X. R. Qi, D. H. Zhang, and Y. S. Zhu, *Phys. Rev. D* **62**, 034003 (2000).
 [40] R.-L. Yang, R.-G. Ping, and H. Chen, *Chin. Phys. Lett.* **31**, 061301 (2014).
 [41] E. Barberio, B. van Eijk, and Z. Was, *Comput. Phys. Commun.* **66**, 115 (1991).
 [42] R.-G. Ping, *Chin. Phys. C* **32**, 599 (2008).
 [43] M. Ablikim *et al.* (BESIII Collaboration), *Phys. Rev. D* **95**, 072010 (2017).
 [44] L. Yan *et al.*, *Chin. Phys. C* **34**, 204 (2010).
 [45] G. Punzi, eConf **C030908**, MODT002 (2003).
 [46] A. Hoecker, P. Speckmayer, J. Stelzer, J. Therhaag, E. von Toerne, and H. Voss, *Proc. Sci. ACAT* (2007) 040 [[arXiv: physics/0703039](https://arxiv.org/abs/physics/0703039)].
 [47] R. Sinkus and T. Voss, *Nucl. Instrum. Methods Phys. Res., Sect. A* **391**, 360 (1997).

- [48] M. Ablikim *et al.* (BESIII Collaboration), *Phys. Rev. D* **81**, 052005 (2010).
 [49] M. Ablikim *et al.* (BESIII Collaboration), *Phys. Rev. D* **87**, 012002 (2013).
 [50] Y. Zhu, *Nucl. Instrum. Methods Phys. Res., Sect. A* **578**, 322 (2007).
 [51] M. Achasov *et al.*, *Front. Phys. (Beijing)* **19**, 14701 (2024).

M. Ablikim,¹ M. N. Achasov,^{4,c} P. Adlarson,⁷⁶ O. Afedulidis,³ X. C. Ai,⁸¹ R. Aliberti,³⁵ A. Amoroso,^{75a,75c} Q. An,^{72,58,a} Y. Bai,⁵⁷ O. Bakina,³⁶ I. Balossino,^{29a} Y. Ban,^{46,h} H.-R. Bao,⁶⁴ V. Batozskaya,^{1,44} K. Begzsuren,³² N. Berger,³⁵ M. Berlowski,⁴⁴ M. Bertani,^{28a} D. Bettoni,^{29a} F. Bianchi,^{75a,75c} E. Bianco,^{75a,75c} A. Bortone,^{75a,75c} I. Boyko,³⁶ R. A. Briere,⁵ A. Brueggemann,⁶⁹ H. Cai,⁷⁷ X. Cai,^{1,58} A. Calcaterra,^{28a} G. F. Cao,^{1,64} N. Cao,^{1,64} S. A. Cetin,^{62a} X. Y. Chai,^{46,h} J. F. Chang,^{1,58} G. R. Che,⁴³ Y. Z. Che,^{1,58,64} G. Chelkov,^{36,b} C. Chen,⁴³ C. H. Chen,⁹ Chao Chen,⁵⁵ G. Chen,¹ H. S. Chen,^{1,64} H. Y. Chen,²⁰ M. L. Chen,^{1,58,64} S. J. Chen,⁴² S. L. Chen,⁴⁵ S. M. Chen,⁶¹ T. Chen,^{1,64} X. R. Chen,^{31,64} X. T. Chen,^{1,64} Y. B. Chen,^{1,58} Y. Q. Chen,³⁴ Z. J. Chen,^{25,i} Z. Y. Chen,^{1,64} S. K. Choi,¹⁰ G. Cibinetto,^{29a} F. Cossio,^{75c} J. J. Cui,⁵⁰ H. L. Dai,^{1,58} J. P. Dai,⁷⁹ A. Dbeyssi,¹⁸ R. E. de Boer,³ D. Dedovich,³⁶ C. Q. Deng,⁷³ Z. Y. Deng,¹ A. Denig,³⁵ I. Denysenko,³⁶ M. Destefanis,^{75a,75c} F. De Mori,^{75a,75c} B. Ding,^{67,1} X. X. Ding,^{46,h} Y. Ding,⁴⁰ Y. Ding,³⁴ J. Dong,^{1,58} L. Y. Dong,^{1,64} M. Y. Dong,^{1,58,64} X. Dong,⁷⁷ M. C. Du,¹ S. X. Du,⁸¹ Y. Y. Duan,⁵⁵ Z. H. Duan,⁴² P. Egorov,^{36,b} Y. H. Fan,⁴⁵ J. Fang,^{1,58} J. Fang,⁵⁹ S. S. Fang,^{1,64} W. X. Fang,¹ Y. Fang,¹ Y. Q. Fang,^{1,58} R. Farinelli,^{29a} L. Fava,^{75b,75c} F. Feldbauer,³ G. Felici,^{28a} C. Q. Feng,^{72,58} J. H. Feng,⁵⁹ Y. T. Feng,^{72,58} M. Fritsch,³ C. D. Fu,¹ J. L. Fu,⁶⁴ Y. W. Fu,^{1,64} H. Gao,⁶⁴ X. B. Gao,⁴¹ Y. N. Gao,^{46,h} Yang Gao,^{72,58} S. Garbolino,^{75c} I. Garzia,^{29a,29b} L. Ge,⁸¹ P. T. Ge,¹⁹ Z. W. Ge,⁴² C. Geng,⁵⁹ E. M. Gersabeck,⁶⁸ A. Gilman,⁷⁰ K. Goetzen,¹³ L. Gong,⁴⁰ W. X. Gong,^{1,58} W. Gradl,³⁵ S. Gramigna,^{29a,29b} M. Greco,^{75a,75c} M. H. Gu,^{1,58} Y. T. Gu,¹⁵ C. Y. Guan,^{1,64} A. Q. Guo,^{31,64} L. B. Guo,⁴¹ M. J. Guo,⁵⁰ R. P. Guo,⁴⁹ Y. P. Guo,^{12,g} A. Guskov,^{36,b} J. Gutierrez,²⁷ K. L. Han,⁶⁴ T. T. Han,¹ F. Hanisch,³ X. Q. Hao,¹⁹ F. A. Harris,⁶⁶ K. K. He,⁵⁵ K. L. He,^{1,64} F. H. Heinsius,³ C. H. Heinz,³⁵ Y. K. Heng,^{1,58,64} C. Herold,⁶⁰ T. Holtmann,³ P. C. Hong,³⁴ G. Y. Hou,^{1,64} X. T. Hou,^{1,64} Y. R. Hou,⁶⁴ Z. L. Hou,¹ B. Y. Hu,⁵⁹ H. M. Hu,^{1,64} J. F. Hu,^{56,j} S. L. Hu,^{12,g} T. Hu,^{1,58,64} Y. Hu,¹ G. S. Huang,^{72,58} K. X. Huang,⁵⁹ L. Q. Huang,^{31,64} X. T. Huang,⁵⁰ Y. P. Huang,¹ Y. S. Huang,⁵⁹ T. Hussain,⁷⁴ F. Hölzken,³ N. Hüsken,³⁵ N. in der Wiesche,⁶⁹ J. Jackson,²⁷ S. Janchiv,³² J. H. Jeong,¹⁰ Q. Ji,¹ Q. P. Ji,¹⁹ W. Ji,^{1,64} X. B. Ji,^{1,64} X. L. Ji,^{1,58} Y. Y. Ji,⁵⁰ X. Q. Jia,⁵⁰ Z. K. Jia,^{72,58} D. Jiang,^{1,64} H. B. Jiang,⁷⁷ P. C. Jiang,^{46,h} S. S. Jiang,³⁹ T. J. Jiang,¹⁶ X. S. Jiang,^{1,58,64} Y. Jiang,⁶⁴ J. B. Jiao,⁵⁰ J. K. Jiao,³⁴ Z. Jiao,²³ S. Jin,⁴² Y. Jin,⁶⁷ M. Q. Jing,^{1,64} X. M. Jing,⁶⁴ T. Johansson,⁷⁶ S. Kabana,³³ N. Kalantar-Nayestanaki,⁶⁵ X. L. Kang,⁹ X. S. Kang,⁴⁰ M. Kavatsyuk,⁶⁵ B. C. Ke,⁸¹ V. Khachatryan,²⁷ A. Khoukaz,⁶⁹ R. Kiuchi,¹ O. B. Kolcu,^{62a} B. Kopf,³ M. Kuessner,³ X. Kui,^{1,64} N. Kumar,²⁶ A. Kupsc,^{44,76} W. Kühn,³⁷ J. J. Lane,⁶⁸ L. Lavezzi,^{75a,75c} T. T. Lei,^{72,58} Z. H. Lei,^{72,58} M. Lellmann,³⁵ T. Lenz,³⁵ C. Li,⁴³ C. Li,⁴⁷ C. H. Li,³⁹ Cheng Li,^{72,58} D. M. Li,⁸¹ F. Li,^{1,58} G. Li,¹ H. B. Li,^{1,64} H. J. Li,¹⁹ H. N. Li,^{56,j} Hui Li,⁴³ J. R. Li,⁶¹ J. S. Li,⁵⁹ K. Li,¹ K. L. Li,¹⁹ L. J. Li,^{1,64} L. K. Li,¹ Lei Li,⁴⁸ M. H. Li,⁴³ P. R. Li,^{38,k,l} Q. M. Li,^{1,64} Q. X. Li,⁵⁰ R. Li,^{17,31} S. X. Li,¹² T. Li,⁵⁰ W. D. Li,^{1,64} W. G. Li,^{1,a} X. Li,^{1,64} X. H. Li,^{72,58} X. L. Li,⁵⁰ X. Y. Li,^{1,64} X. Z. Li,⁵⁹ Y. G. Li,^{46,h} Z. J. Li,⁵⁹ Z. Y. Li,⁷⁹ C. Liang,⁴² H. Liang,^{1,64} H. Liang,^{72,58} Y. F. Liang,⁵⁴ Y. T. Liang,^{31,64} G. R. Liao,¹⁴ Y. P. Liao,^{1,64} J. Libby,²⁶ A. Limphirat,⁶⁰ C. C. Lin,⁵⁵ D. X. Lin,^{31,64} T. Lin,¹ B. J. Liu,¹ B. X. Liu,⁷⁷ C. Liu,³⁴ C. X. Liu,¹ F. Liu,¹ F. H. Liu,⁵³ Feng Liu,⁶ G. M. Liu,^{56,j} H. Liu,^{38,k,l} H. B. Liu,¹⁵ H. H. Liu,¹ H. M. Liu,^{1,64} Huihui Liu,²¹ J. B. Liu,^{72,58} J. Y. Liu,^{1,64} K. Liu,^{38,k,l} K. Y. Liu,⁴⁰ Ke Liu,²² L. Liu,^{72,58} L. C. Liu,⁴³ Lu Liu,⁴³ M. H. Liu,^{12,g} P. L. Liu,¹ Q. Liu,⁶⁴ S. B. Liu,^{72,58} T. Liu,^{12,g} W. K. Liu,⁴³ W. M. Liu,^{72,58} X. Liu,^{38,k,l} X. Liu,³⁹ Y. Liu,⁸¹ Y. Liu,^{38,k,l} Y. B. Liu,⁴³ Z. A. Liu,^{1,58,64} Z. D. Liu,⁹ Z. Q. Liu,⁵⁰ X. C. Lou,^{1,58,64} F. X. Lu,⁵⁹ H. J. Lu,²³ J. G. Lu,^{1,58} X. L. Lu,¹ Y. Lu,⁷ Y. P. Lu,^{1,58} Z. H. Lu,^{1,64} C. L. Luo,⁴¹ J. R. Luo,⁵⁹ M. X. Luo,⁸⁰ T. Luo,^{12,g} X. L. Luo,^{1,58} X. R. Lyu,⁶⁴ Y. F. Lyu,⁴³ F. C. Ma,⁴⁰ H. Ma,⁷⁹ H. L. Ma,¹ J. L. Ma,^{1,64} L. L. Ma,⁵⁰ L. R. Ma,⁶⁷ M. M. Ma,^{1,64} Q. M. Ma,¹ R. Q. Ma,^{1,64} T. Ma,^{72,58} X. T. Ma,^{1,64} X. Y. Ma,^{1,58} Y. M. Ma,³¹ F. E. Maas,¹⁸ I. MacKay,⁷⁰ M. Maggiora,^{75a,75c} S. Malde,⁷⁰ Y. J. Mao,^{46,h} Z. P. Mao,¹ S. Marcello,^{75a,75c} Z. X. Meng,⁶⁷ J. G. Messchendorp,^{13,65} G. Mezzadri,^{29a} H. Miao,^{1,64} T. J. Min,⁴² R. E. Mitchell,²⁷ X. H. Mo,^{1,58,64} B. Moses,²⁷ N. Yu. Muchnoi,^{4,c} J. Muskalla,³⁵ Y. Nefedov,³⁶ F. Nerling,^{18,e} L. S. Nie,²⁰ I. B. Nikolaev,^{4,c} Z. Ning,^{1,58} S. Nisar,^{11,m} Q. L. Niu,^{38,k,l} W. D. Niu,⁵⁵ Y. Niu,⁵⁰ S. L. Olsen,⁶⁴ S. L. Olsen,^{10,64} Q. Ouyang,^{1,58,64} S. Pacetti,^{28b,28c} X. Pan,⁵⁵ Y. Pan,⁵⁷ A. Pathak,³⁴ Y. P. Pei,^{72,58} M. Pelizaeus,³ H. P. Peng,^{72,58} Y. Y. Peng,^{38,k,l} K. Peters,^{13,e} J. L. Ping,⁴¹ R. G. Ping,^{1,64} S. Plura,³⁵ V. Prasad,³³ F. Z. Qi,¹ H. Qi,^{72,58} H. R. Qi,⁶¹ M. Qi,⁴² T. Y. Qi,^{12,g} S. Qian,^{1,58} W. B. Qian,⁶⁴ C. F. Qiao,⁶⁴ X. K. Qiao,⁸¹ J. J. Qin,⁷³ L. Q. Qin,¹⁴ L. Y. Qin,^{72,58} X. P. Qin,^{12,g} X. S. Qin,⁵⁰ Z. H. Qin,^{1,58} J. F. Qiu,¹ Z. H. Qu,⁷³

C. F. Redmer,³⁵ K. J. Ren,³⁹ A. Rivetti,^{75c} M. Rolo,^{75c} G. Rong,^{1,64} Ch. Rosner,¹⁸ M. Q. Ruan,^{1,58} S. N. Ruan,⁴³ N. Salone,⁴⁴
 A. Sarantsev,^{36,d} Y. Schelhaas,³⁵ K. Schoenning,⁷⁶ M. Scodreggio,^{29a} K. Y. Shan,^{12,g} W. Shan,²⁴ X. Y. Shan,^{72,58}
 Z. J. Shang,^{38,k,l} J. F. Shangguan,¹⁶ L. G. Shao,^{1,64} M. Shao,^{72,58} C. P. Shen,^{12,g} H. F. Shen,^{1,8} W. H. Shen,⁶⁴ X. Y. Shen,^{1,64}
 B. A. Shi,⁶⁴ H. Shi,^{72,58} H. C. Shi,^{72,58} J. L. Shi,^{12,g} J. Y. Shi,¹ Q. Q. Shi,⁵⁵ S. Y. Shi,⁷³ X. Shi,^{1,58} J. J. Song,¹⁹ T. Z. Song,⁵⁹
 W. M. Song,^{34,l} Y. J. Song,^{12,g} Y. X. Song,^{46,h,n} S. Sosio,^{75a,75c} S. Spataro,^{75a,75c} F. Stieler,³⁵ S. S. Su,⁴⁰ Y. J. Su,⁶⁴ G. B. Sun,⁷⁷
 G. X. Sun,¹ H. Sun,⁶⁴ H. K. Sun,¹ J. F. Sun,¹⁹ K. Sun,⁶¹ L. Sun,⁷⁷ S. S. Sun,^{1,64} T. Sun,^{51,f} W. Y. Sun,³⁴ Y. Sun,⁹ Y. J. Sun,^{72,58}
 Y. Z. Sun,¹ Z. Q. Sun,^{1,64} Z. T. Sun,⁵⁰ C. J. Tang,⁵⁴ G. Y. Tang,¹ J. Tang,⁵⁹ M. Tang,^{72,58} Y. A. Tang,⁷⁷ L. Y. Tao,⁷³
 Q. T. Tao,^{25,i} M. Tat,⁷⁰ J. X. Teng,^{72,58} V. Thoren,⁷⁶ W. H. Tian,⁵⁹ Y. Tian,^{31,64} Z. F. Tian,⁷⁷ I. Uman,^{62b} Y. Wan,⁵⁵
 S. J. Wang,⁵⁰ B. Wang,¹ B. L. Wang,⁶⁴ Bo Wang,^{72,58} D. Y. Wang,^{46,h} F. Wang,⁷³ H. J. Wang,^{38,k,l} J. J. Wang,⁷⁷ J. P. Wang,⁵⁰
 K. Wang,^{1,58} L. L. Wang,¹ M. Wang,⁵⁰ N. Y. Wang,⁶⁴ S. Wang,^{38,k,l} S. Wang,^{12,g} T. Wang,^{12,g} T. J. Wang,⁴³ W. Wang,⁷³
 W. Wang,⁵⁹ W. P. Wang,^{35,58,72,o} X. Wang,^{46,h} X. F. Wang,^{38,k,l} X. J. Wang,³⁹ X. L. Wang,^{12,g} X. N. Wang,¹ Y. Wang,⁶¹
 Y. D. Wang,⁴⁵ Y. F. Wang,^{1,58,64} Y. L. Wang,¹⁹ Y. N. Wang,⁴⁵ Y. Q. Wang,¹ Yaqian Wang,¹⁷ Yi Wang,⁶¹ Z. Wang,^{1,58}
 Z. L. Wang,⁷³ Z. Y. Wang,^{1,64} Ziyi Wang,⁶⁴ D. H. Wei,¹⁴ F. Weidner,⁶⁹ S. P. Wen,¹ Y. R. Wen,³⁹ U. Wiedner,³ G. Wilkinson,⁷⁰
 M. Wolke,⁷⁶ L. Wollenberg,³ C. Wu,³⁹ J. F. Wu,^{1,8} L. H. Wu,¹ L. J. Wu,^{1,64} X. Wu,^{12,g} X. H. Wu,³⁴ Y. Wu,^{72,58} Y. H. Wu,⁵⁵
 Y. J. Wu,³¹ Z. Wu,^{1,58} L. Xia,^{72,58} X. M. Xian,³⁹ B. H. Xiang,^{1,64} T. Xiang,^{46,h} D. Xiao,^{38,k,l} G. Y. Xiao,⁴² S. Y. Xiao,¹
 Y. L. Xiao,^{12,g} Z. J. Xiao,⁴¹ C. Xie,⁴² X. H. Xie,^{46,h} Y. Xie,⁵⁰ Y. G. Xie,^{1,58} Y. H. Xie,⁶ Z. P. Xie,^{72,58} T. Y. Xing,^{1,64}
 C. F. Xu,^{1,64} C. J. Xu,⁵⁹ G. F. Xu,¹ H. Y. Xu,^{67,2,p} M. Xu,^{72,58} Q. J. Xu,¹⁶ Q. N. Xu,³⁰ W. Xu,¹ W. L. Xu,⁶⁷ X. P. Xu,⁵⁵ Y. Xu,⁴⁰
 Y. C. Xu,⁷⁸ Z. S. Xu,⁶⁴ F. Yan,^{12,g} L. Yan,^{12,g} W. B. Yan,^{72,58} W. C. Yan,⁸¹ X. Q. Yan,^{1,64} H. J. Yang,^{51,f} H. L. Yang,³⁴
 H. X. Yang,¹ T. Yang,¹ Y. Yang,^{12,g} Y. F. Yang,^{1,64} Y. F. Yang,⁴³ Y. X. Yang,^{1,64} Z. W. Yang,^{38,k,l} Z. P. Yao,⁵⁰ M. Ye,^{1,58}
 M. H. Ye,⁸ J. H. Yin,¹ Junhao Yin,⁴³ Z. Y. You,⁵⁹ B. X. Yu,^{1,58,64} C. X. Yu,⁴³ G. Yu,^{1,64} J. S. Yu,^{25,i} M. C. Yu,⁴⁰ T. Yu,⁷³
 X. D. Yu,^{46,h} Y. C. Yu,⁸¹ C. Z. Yuan,^{1,64} J. Yuan,³⁴ J. Yuan,⁴⁵ L. Yuan,² S. C. Yuan,^{1,64} Y. Yuan,^{1,64} Z. Y. Yuan,⁵⁹ C. X. Yue,³⁹
 A. A. Zafar,⁷⁴ F. R. Zeng,⁵⁰ S. H. Zeng,^{63a,63b,63c,63d} X. Zeng,^{12,g} Y. Zeng,^{25,i} Y. J. Zeng,⁵⁹ Y. J. Zeng,^{1,64} X. Y. Zhai,³⁴
 Y. C. Zhai,⁵⁰ Y. H. Zhan,⁵⁹ A. Q. Zhang,^{1,64} B. L. Zhang,^{1,64} B. X. Zhang,¹ D. H. Zhang,⁴³ G. Y. Zhang,¹⁹ H. Zhang,⁸¹
 H. Zhang,^{72,58} H. C. Zhang,^{1,58,64} H. H. Zhang,³⁴ H. H. Zhang,⁵⁹ H. Q. Zhang,^{1,58,64} H. R. Zhang,^{72,58} H. Y. Zhang,^{1,58}
 J. Zhang,⁵⁹ J. Zhang,⁸¹ J. J. Zhang,⁵² J. L. Zhang,²⁰ J. Q. Zhang,⁴¹ J. S. Zhang,^{12,g} J. W. Zhang,^{1,58,64} J. X. Zhang,^{38,k,l}
 J. Y. Zhang,¹ J. Z. Zhang,^{1,64} Jianyu Zhang,⁶⁴ L. M. Zhang,⁶¹ Lei Zhang,⁴² P. Zhang,^{1,64} Q. Y. Zhang,³⁴ R. Y. Zhang,^{38,k,l}
 S. H. Zhang,^{1,64} Shulei Zhang,^{25,i} X. M. Zhang,¹ X. Y. Zhang,⁴⁰ X. Y. Zhang,⁵⁰ Y. Zhang,¹ Y. Zhang,⁷³ Y. T. Zhang,⁸¹
 Y. H. Zhang,^{1,58} Y. M. Zhang,³⁹ Yan Zhang,^{72,58} Z. D. Zhang,¹ Z. H. Zhang,¹ Z. L. Zhang,³⁴ Z. Y. Zhang,⁷⁷ Z. Y. Zhang,⁴³
 Z. Z. Zhang,⁴⁵ G. Zhao,¹ J. Y. Zhao,^{1,64} J. Z. Zhao,^{1,58} L. Zhao,¹ Lei Zhao,^{72,58} M. G. Zhao,⁴³ N. Zhao,⁷⁹ R. P. Zhao,⁶⁴
 S. J. Zhao,⁸¹ Y. B. Zhao,^{1,58} Y. X. Zhao,^{31,64} Z. G. Zhao,^{72,58} A. Zhemchugov,^{36,b} B. Zheng,⁷³ B. M. Zheng,³⁴ J. P. Zheng,^{1,58}
 W. J. Zheng,^{1,64} Y. H. Zheng,⁶⁴ B. Zhong,⁴¹ X. Zhong,⁵⁹ H. Zhou,⁵⁰ J. Y. Zhou,³⁴ L. P. Zhou,^{1,64} S. Zhou,⁶ X. Zhou,⁷⁷
 X. K. Zhou,⁶ X. R. Zhou,^{72,58} X. Y. Zhou,³⁹ Y. Z. Zhou,^{12,g} Z. C. Zhou,²⁰ A. N. Zhu,⁶⁴ J. Zhu,⁴³ K. Zhu,¹ K. J. Zhu,^{1,58,64}
 K. S. Zhu,^{12,g} L. Zhu,³⁴ L. X. Zhu,⁶⁴ S. H. Zhu,⁷¹ T. J. Zhu,^{12,g} W. D. Zhu,⁴¹ Y. C. Zhu,^{72,58}
 Z. A. Zhu,^{1,64} J. H. Zou,¹ and J. Zu^{72,58}

(BESIII Collaboration)

¹*Institute of High Energy Physics, Beijing 100049, People's Republic of China*²*Beihang University, Beijing 100191, People's Republic of China*³*Bochum Ruhr-University, D-44780 Bochum, Germany*⁴*Budker Institute of Nuclear Physics SB RAS (BINP), Novosibirsk 630090, Russia*⁵*Carnegie Mellon University, Pittsburgh, Pennsylvania 15213, USA*⁶*Central China Normal University, Wuhan 430079, People's Republic of China*⁷*Central South University, Changsha 410083, People's Republic of China*⁸*China Center of Advanced Science and Technology, Beijing 100190, People's Republic of China*⁹*China University of Geosciences, Wuhan 430074, People's Republic of China*¹⁰*Chung-Ang University, Seoul, 06974, Republic of Korea*¹¹*COMSATS University Islamabad, Lahore Campus, Defence Road, Off Raiwind Road, 54000 Lahore, Pakistan*¹²*Fudan University, Shanghai 200433, People's Republic of China*¹³*GSI Helmholtzcentre for Heavy Ion Research GmbH, D-64291 Darmstadt, Germany*¹⁴*Guangxi Normal University, Guilin 541004, People's Republic of China*

- ¹⁵Guangxi University, Nanning 530004, People's Republic of China
- ¹⁶Hangzhou Normal University, Hangzhou 310036, People's Republic of China
- ¹⁷Hebei University, Baoding 071002, People's Republic of China
- ¹⁸Helmholtz Institute Mainz, Staudinger Weg 18, D-55099 Mainz, Germany
- ¹⁹Henan Normal University, Xinxiang 453007, People's Republic of China
- ²⁰Henan University, Kaifeng 475004, People's Republic of China
- ²¹Henan University of Science and Technology, Luoyang 471003, People's Republic of China
- ²²Henan University of Technology, Zhengzhou 450001, People's Republic of China
- ²³Huangshan College, Huangshan 245000, People's Republic of China
- ²⁴Hunan Normal University, Changsha 410081, People's Republic of China
- ²⁵Hunan University, Changsha 410082, People's Republic of China
- ²⁶Indian Institute of Technology Madras, Chennai 600036, India
- ²⁷Indiana University, Bloomington, Indiana 47405, USA
- ^{28a}INFN Laboratori Nazionali di Frascati, I-00044 Frascati, Italy
- ^{28b}INFN Sezione di Perugia, I-06100 Perugia, Italy
- ^{28c}University of Perugia, I-06100 Perugia, Italy
- ^{29a}INFN Sezione di Ferrara, I-44122 Ferrara, Italy
- ^{29b}University of Ferrara, I-44122 Ferrara, Italy
- ³⁰Inner Mongolia University, Hohhot 010021, People's Republic of China
- ³¹Institute of Modern Physics, Lanzhou 730000, People's Republic of China
- ³²Institute of Physics and Technology, Peace Avenue 54B, Ulaanbaatar 13330, Mongolia
- ³³Instituto de Alta Investigación, Universidad de Tarapacá, Casilla 7D, Arica 1000000, Chile
- ³⁴Jilin University, Changchun 130012, People's Republic of China
- ³⁵Johannes Gutenberg University of Mainz, Johann-Joachim-Becher-Weg 45, D-55099 Mainz, Germany
- ³⁶Joint Institute for Nuclear Research, 141980 Dubna, Moscow region, Russia
- ³⁷Justus-Liebig-Universitaet Giessen, II. Physikalisches Institut, Heinrich-Buff-Ring 16, D-35392 Giessen, Germany
- ³⁸Lanzhou University, Lanzhou 730000, People's Republic of China
- ³⁹Liaoning Normal University, Dalian 116029, People's Republic of China
- ⁴⁰Liaoning University, Shenyang 110036, People's Republic of China
- ⁴¹Nanjing Normal University, Nanjing 210023, People's Republic of China
- ⁴²Nanjing University, Nanjing 210093, People's Republic of China
- ⁴³Nankai University, Tianjin 300071, People's Republic of China
- ⁴⁴National Centre for Nuclear Research, Warsaw 02-093, Poland
- ⁴⁵North China Electric Power University, Beijing 102206, People's Republic of China
- ⁴⁶Peking University, Beijing 100871, People's Republic of China
- ⁴⁷Qufu Normal University, Qufu 273165, People's Republic of China
- ⁴⁸Renmin University of China, Beijing 100872, People's Republic of China
- ⁴⁹Shandong Normal University, Jinan 250014, People's Republic of China
- ⁵⁰Shandong University, Jinan 250100, People's Republic of China
- ⁵¹Shanghai Jiao Tong University, Shanghai 200240, People's Republic of China
- ⁵²Shanxi Normal University, Linfen 041004, People's Republic of China
- ⁵³Shanxi University, Taiyuan 030006, People's Republic of China
- ⁵⁴Sichuan University, Chengdu 610064, People's Republic of China
- ⁵⁵Soochow University, Suzhou 215006, People's Republic of China
- ⁵⁶South China Normal University, Guangzhou 510006, People's Republic of China
- ⁵⁷Southeast University, Nanjing 211100, People's Republic of China
- ⁵⁸State Key Laboratory of Particle Detection and Electronics, Beijing 100049, Hefei 230026, People's Republic of China
- ⁵⁹Sun Yat-Sen University, Guangzhou 510275, People's Republic of China
- ⁶⁰Suranaree University of Technology, University Avenue 111, Nakhon Ratchasima 30000, Thailand
- ⁶¹Tsinghua University, Beijing 100084, People's Republic of China
- ^{62a}Turkish Accelerator Center Particle Factory Group, Istinye University, 34010 Istanbul, Turkey
- ^{62b}Near East University, Nicosia, North Cyprus, 99138, Mersin 10, Turkey
- ^{63a}University of Bristol, H H Wills Physics Laboratory
Tyndall Avenue
- ^{63b}Tyndall Avenue
- ^{63c}Bristol
- ^{63d}BS8 1TL
- ⁶⁴University of Chinese Academy of Sciences, Beijing 100049, People's Republic of China
- ⁶⁵University of Groningen, NL-9747 AA Groningen, The Netherlands

⁶⁶*University of Hawaii, Honolulu, Hawaii 96822, USA*

⁶⁷*University of Jinan, Jinan 250022, People's Republic of China*

⁶⁸*University of Manchester, Oxford Road, Manchester M13 9PL, United Kingdom*

⁶⁹*University of Muenster, Wilhelm-Klemm-Strasse 9, 48149 Muenster, Germany*

⁷⁰*University of Oxford, Keble Road, Oxford OX13RH, United Kingdom*

⁷¹*University of Science and Technology Liaoning, Anshan 114051, People's Republic of China*

⁷²*University of Science and Technology of China, Hefei 230026, People's Republic of China*

⁷³*University of South China, Hengyang 421001, People's Republic of China*

⁷⁴*University of the Punjab, Lahore-54590, Pakistan*

^{75a}*University of Turin and INFN, University of Turin, I-10125 Turin, Italy*

^{75b}*University of Eastern Piedmont, I-15121 Alessandria, Italy*

^{75c}*INFN, I-10125 Turin, Italy*

⁷⁶*Uppsala University, Box 516, SE-75120 Uppsala, Sweden*

⁷⁷*Wuhan University, Wuhan 430072, People's Republic of China*

⁷⁸*Yantai University, Yantai 264005, People's Republic of China*

⁷⁹*Yunnan University, Kunming 650500, People's Republic of China*

⁸⁰*Zhejiang University, Hangzhou 310027, People's Republic of China*

⁸¹*Zhengzhou University, Zhengzhou 450001, People's Republic of China*

^aDeceased.

^bAlso at the Moscow Institute of Physics and Technology, Moscow 141700, Russia.

^cAlso at the Novosibirsk State University, Novosibirsk, 630090, Russia.

^dAlso at the NRC "Kurchatov Institute", PNPI, 188300, Gatchina, Russia.

^eAlso at Goethe University Frankfurt, 60323 Frankfurt am Main, Germany.

^fAlso at Key Laboratory for Particle Physics, Astrophysics and Cosmology, Ministry of Education; Shanghai Key Laboratory for Particle Physics and Cosmology; Institute of Nuclear and Particle Physics, Shanghai 200240, People's Republic of China.

^gAlso at Key Laboratory of Nuclear Physics and Ion-beam Application (MOE) and Institute of Modern Physics, Fudan University, Shanghai 200443, People's Republic of China.

^hAlso at State Key Laboratory of Nuclear Physics and Technology, Peking University, Beijing 100871, People's Republic of China.

ⁱAlso at School of Physics and Electronics, Hunan University, Changsha 410082, China.

^jAlso at Guangdong Provincial Key Laboratory of Nuclear Science, Institute of Quantum Matter, South China Normal University, Guangzhou 510006, China.

^kAlso at MOE Frontiers Science Center for Rare Isotopes, Lanzhou University, Lanzhou 730000, People's Republic of China.

^lAlso at Lanzhou Center for Theoretical Physics, Lanzhou University, Lanzhou 730000, People's Republic of China.

^mAlso at the Department of Mathematical Sciences, IBA, Karachi 75270, Pakistan.

ⁿAlso at Ecole Polytechnique Federale de Lausanne (EPFL), CH-1015 Lausanne, Switzerland.

^oAlso at Helmholtz Institute Mainz, Staudinger Weg 18, D-55099 Mainz, Germany.

^pAlso at School of Physics, Beihang University, Beijing 100191, China.